Journal of Thermal Analysis, Vol. 28 (1983) 237–248

LOW AND HIGH-YIELD ISOTACTIC POLYPROPYLENE
Isothermal crystallization from the melt

M. Avella, E. Martuscelli and *M. Pracella* *

ISTITUTO DI RICERCHE SU TECNOLOGIA DEI POLIMERI E REOLOGIA DEL CNR, 80072 ARCOFELICE (NA), *CENTRO STUDI DEI PROCESSI IONICI E DELLA PROPRIETÀ DEI SISTEMI MACROMOLECOLARI DEL CNR, INGEGNERIA CHIMICA, UNIVERSITÀ DE PISA, 56100 PISA, ITALY

The crystallization and melting behaviour of isotactic polypropylene (iPP) samples synthetized with different catalyst systems (low and high-yield) have been studied by differential scanning calorimetry and optical microscopy. The isothermal crystallization rates from the melt have been found to depend on the catalyst system employed and on the isotacticity index of the sample. Moreover, for low-yield iPP, Avrami analysis of the overall kinetics has provided evidence of the presence of secondary crystallization phenomena. The values of the equilibrium melting point, energy of nucleation and surface energy of folding of iPP lamellar crystals have been calculated according to the 'Kinetic theories' of polymer crystallization. The observed variation of such thermodynamic parameters for the various iPP samples has been accounted for by the amount and type of configurational irregularities present along the chains and by the differences in the molecular weight distribution.

The presence of configurational irregularities in isotactic polypropylene (iPP) chains influences the morphological parameters, the thermal behaviour, and the rheological and mechanical properties of this polymer [1, 2]. The most recent methods of iPP industrial production are based on the employment of new (high-yield) catalyst systems which yield materials with a controlled distribution of the average molecular weight and a chain stereoregularity giving iPP properties different from those shown by the polymer obtained with traditional (low-yield) catalyst systems.

The main aim of the present research is to study the kinetics of isothermal crystallization from the melt, and the melting behaviour of (low- and high-yield) iPP samples with different isotacticity indices, in order to analyze the influence of the chain stereoregularity on the morphological, kinetic and thermodynamic parameters controlling the crystallization processes of such materials [3].

Materials and experimental procedures

Four different samples of iPP (supplied by Centro Ricerche G. Natta, Montepolimeri) were examined: one of these, Moplen S, was obtained in the traditional way

with a catalyst system denotes 'low-yield', while the remaining three samples were synthetized with 'high-yield' catalyst systems. The characteristics of all samples are reported in Table 1.

Table 1 Isotacticity index and physical–chemical characteristics of iPP samples obtained by low- and high-yield catalyst systems

Sample	Catalyst system	Heptane extract, wt %	Isotacticity index, %	Viscosity, dl/g	Melt flow index, g/10	Melting point, K	Crystallinity, %
Moplen S	Low-yield	2.5	97.5	2.35	2.1	436.6	64
H97.5	High-yield	2.5	97.5	2.52	1.6	435.7	68
H96.0	High-yield	4.0	96.0	2.43	1.8	434.5	68
H90.0	High-yield	10.0	90.0	2.47	1.6	433.4	57

The value of the isotacticity index was determined from the weight percentage of polymer undissolved in heptane.

The kinetics of isothermal crystallization from the melt for all samples were studied by using a Perkin–Elmer DSC-2 differential scanning calorimeter operating under a N_2 atmosphere. The following procedure was employed: the samples were kept for 10 minutes at 190° and then rapidly cooled to the crystallization temperature T_c.

The heat (dH/dt) evolved during the isothermal crystallization was recorded as a function of time t, and the weight fraction X_t of material crystallized after time t was determined via the relation:

$$X_t = \int_0^t \left(\frac{dH}{dt}\right) dt \int_0^\infty \left(\frac{dH}{dt}\right) dt$$

where the first integral is the crystallization heat evolved at time t, and the second integral is the total crystallization heat for $t = \infty$.

The melting temperature T'_m and the apparent enthalpy of fusion ΔH_f^* of each sample after isothermal crystallization at T_c were measured from the maxima and the areas, respectively, of the DSC endotherms obtained by heating the samples directly from T_c to T'_m at heating rates of 20 degree/min. Higher scan rates (40 or 80 degree/min) were also used in order to check the influence of the heating rate on the melting point. The temperatures of the calorimeter were calibrated against the melting points of high-purity standards under different heating conditions, with a precision of ±0.2 degrees.

The crystallinity fraction X_c of the samples was determined at each T_c as the ratio of ΔH_f^* to the fusion enthalpy ΔH_f of a sample with 100% crystallinity, taken as 50 cal/g (209 kJ/kg) [4].

The morphology and the radial growth rates of iPP spherulites isothermally crystallizing at various temperatures T_c were studied by examining thin films of the samples with a Reichert polarizing optical microscope equipped with a Mettler hot stage. The radial growth rates G were measured from the linear variation of the spherulite radius as a function of the crystallization time at T_c.

Results and discussion

Overall crystallization rates

The iPP samples were isothermally crystallized from the melt in the temperature range from 396 K to 407 K.

On decrease of the isotacticity index, the overall crystallization rate becomes progressively slower, as shown in Fig. 1, where the values of the half-time of crystallization $t_{0.5}$, defined as the time taken for half of the crystallinity to develop, are plotted against T_c for all the examined polymers. From this plot it emerges that at constant T_c the overall crystallization rate of Moplen is higher than those of high-yield samples, while further the crystallization rate of iPP decreases with decrease of the isotacticity index. Similar results were earlier found in the case of fractions of iPP's with different degrees of stereoregularity (on the basis of C-13 NMR analysis),

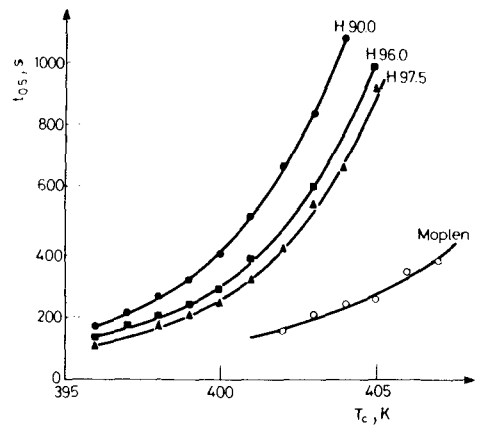

Fig. 1 Half-time of crystallization $t_{0.5}$ of low-yield iPP (Moplen) and high-yield iPPs with different isotacticity indices (H97.5, H96.0, H90.0) as a function of isothermal crystallization temperature T_c

synthetized by using titanium-based catalysts and fractionated by successive extractions with hydrocarbon solvents or by isothermal crystallization from solution at different temperatures [1].

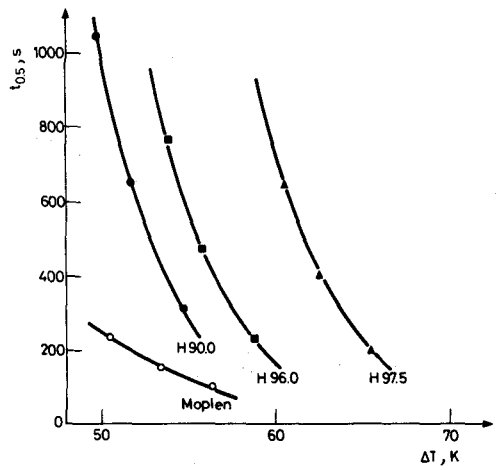

Fig. 2 Half-time of crystallization $t_{0.5}$ of low-yield iPP (Moplen) and high-yield iPPs (H97.5, H96.0, H90.0) *vs.* the undercooling ΔT

Figure 2 shows the variation of the half-time of crystallization with the undercooling $\Delta T = T_m - T_c$, where T_m is the equilibrium melting temperature of each sample. It may be noted that at the same ΔT the crystallization rate of the high-yield iPP decreases with the increase of the isotacticity index, analogously to what was observed in blends of isotactic and atactic polypropylenes, for which the spherulite growth rate at constant undercooling increases with the content of atactic polymer in the blend [2, 5].

The analysis of the crystallization kinetics has been performed following the Avrami equation [6]:

$$1 - X_t = \exp(-K_n t^n) \tag{1}$$

where K_n ($= \ln 2/t_{0.5}^n$) is the kinetic constant and n is a parameter dependent on the nucleation type and on the geometry of the growing crystals. Values of K_n and n have been calculated at each T_c from the intercept and the slope, respectively, of the linear plots of the quantity $\log|\log(1 - X_t)|$ *vs.* $\log t$ (see Table 2).

As shown in Figs 3a, b, such plots for the high-yield iPP samples are single straight lines over the whole temperature range explored, with slopes varying from 2.5 to 2.0, corresponding closely to a heterogeneously nucleated three-dimensional growth of the crystals [6].

In contrast, as shown in Fig. 3c, abrupt changes in the slopes of the Avrami plots are observed in the case of Moplen at values of the crystallization time which increase with increasing T_c. The exponent n first ranges between 2.5 and 2.0, as for the high-yield samples; then, at larger times, it falls to values between 1.7 and 1.0 characteristic

of a one-dimensional growth of crystals. This behaviour is a clear indication that, during the isothermal crystallization of the low-yield iPP, two distinct processes are present: a 'primary crystallization' characterized by the growth of the fibrils of the

Table 2 Values of half-time of crystallization $t_{0.5}$, Avrami exponent n, kinetic constant K_n and spherulite growth rate G of low- and high-yield iPP samples at various temperatures T_c

Sample	T_c, K	$t_{0.5}$, sec	n	K_n, sec^{-n}	G, μm/sec
Moplen S	401	130	2.5/1.3	2.5×10^{-6}	0.142
	402	154	–	–	
	403	204	2.0/1.0	1.0×10^{-5}	
	404	235	2.3/1.5	9.0×10^{-6}	
	405	252	2.3/1.7	4.7×10^{-6}	0.061
	406	342	2.2/1.6	4.2×10^{-6}	
	407	378	2.0/1.0	7.3×10^{-7}	
	408	–	–	–	0.036
H97.5	396	106	2.5	1.3×10^{-5}	
	397	135	2.4	5.1×10^{-6}	
	398	164	2.5	3.7×10^{-6}	
	399	202	2.5	2.3×10^{-6}	
	400	234	2.5	1.6×10^{-6}	
	401	315	2.5	6.6×10^{-6}	0.138
	402	412	2.5	2.6×10^{-7}	
	403	551	2.5	1.5×10^{-7}	
	404	667	2.3	3.9×10^{-7}	
	405	923	2.5	3.6×10^{-8}	0.073
	408	–	–	–	0.032
H96.0	396	130	2.0	4.5×10^{-5}	
	397	163	2.1	2.0×10^{-5}	
	398	193	2.1	1.6×10^{-5}	
	399	232	2.1	1.1×10^{-5}	
	400	279	2.0	1.0×10^{-5}	
	401	375	2.2	1.8×10^{-6}	0.118
	403	612	2.4	1.5×10^{-7}	0.093
	405	993	2.4	4.7×10^{-8}	0.052
	408	–	–	–	0.025
H90.0	396	169	2.2	1.1×10^{-5}	
	397	208	2.3	6.3×10^{-6}	
	398	258	2.4	1.3×10^{-6}	
	399	320	2.5	5.5×10^{-7}	
	400	394	2.4	4.8×10^{-7}	
	401	510	2.6	9.1×10^{-7}	0.113
	402	673	2.5	8.9×10^{-8}	
	403	840	2.5	6.0×10^{-8}	
	404	1080	2.4	3.9×10^{-8}	0.043
	408	–	–	–	0.023

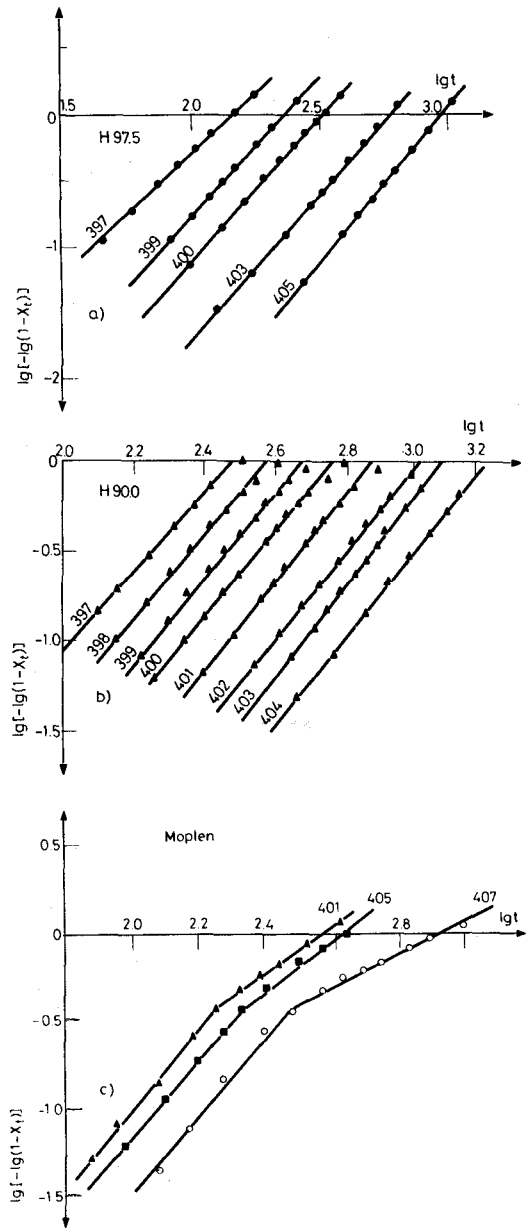

Fig. 3 Avrami plots at various crystallization temperatures, according to Eq. (1). (a) high-yield iPP H97.5, (b) high-yield iPP H90.0, (c) low-yield iPP Moplen. The values of the slopes and the intercepts of the straight lines are reported in Table 2

spherulites, and a 'secondary crystallization', which is active at larger crystallization times, related to the crystallization of more defective molecules in the intraspherulitic or interfibrillar regions, and to phenomena of partial melting and recrystallization at T_c [7].

Effects of secondary crystallization were also observed in the case of iPP fractions with low-degrees of stereoregularity [2]. Accordingly, the observation of such phenomena during the crystallization of Moplen should indicate that this polymer mainly contains molecules with a lower configurational regularity, while in the case of high-yield samples the crystallizing molecules probably have the same average stereochemical composition with a degree of stereoregularity which does not give rise to relevant secondary crystallization processes. Consequently, the variations observed in the values of the kinetic parameters with variation of the isotacticity index of the high-yield samples must be mainly ascribed to differences in the amount of atactic molecules in such materials. Thus, it is possible to suggest from this analysis that the two catalyst systems considered give iPP samples which differ not only in their stereoregularity degree, but also in their atactic content.

Melting behaviour

DSC curves of high-yield samples present only one fusion peak, independently of the heating rate and crystallization temperature. In contrast, the curves of the low-yield iPP generally show a large fusion peak with a shoulder at lower temperature. The latter is clearly distinct and resolvable from the former in Moplen samples crystallized at $T_c < 400$ K, where the crystallization is very fast and does not occur under isothermal conditions.

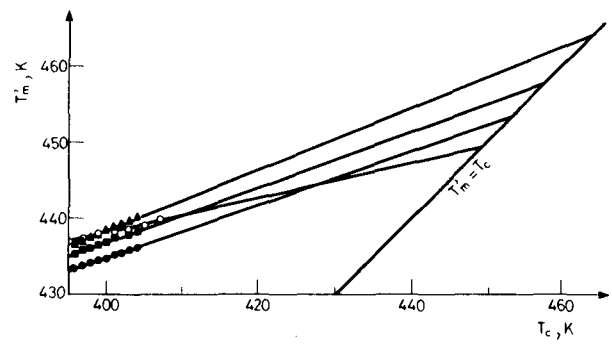

Fig. 4 Variation of the melting temperature T'_m of low-yield iPP (Moplen) and high-yield iPPs (H97.5, H96.0, H90.0) with the crystallization temperature T_c. The extrapolation of the experimental points to the line $T'_m = T_c$ determines the value of the equilibrium melting temperature T_m of each sample (see Table 3). ○ Moplen, ▲ H97.5, ■ H96.0, ● H90.0

As shown in Fig. 4, the melting temperatures T'_m of the various samples crystallized at the same T_c increase with increase of the isotacticity index and, for each sample, increase linearly with T_c according to the relation [8].

$$T'_m = T_m \frac{\gamma - 1}{\gamma} + \frac{T_c}{\gamma} \tag{2}$$

where T_m is the equilibrium melting temperature and γ is a constant determined by the ratio between the final thickness of the crystalline lamellae of the spherulites and the initial thickness of the nuclei at the same temperature. In Table 3 the values of T_m and γ, calculated respectively by extrapolation of T'_m to the line $T'_m = \bar{T}_c$ and from the slopes of Eq. (2), are reported for all the samples. In the case of high-yield iPP the values of T_m decrease with decreasing isotacticity index, while the T_m extrapolated for Moplen is unusually lower than those of the other samples in spite of its high isotacticity index [1, 2]. A possible explanation of this effect is that, though the

Table 3 Values of the equilibrium melting temperature T_m, of the slope γ in the plots of T'_m *vs.* T_c for various low- and high-yield iPP samples

Sample	T_m, K	γ	σ_e, J/m^2
Moplen S	449.6	4.3	55×10^{-3}
H97.5	464.5	2.5	166×10^{-3}
H96.0	457.7	2.7	122×10^{-3}
H90.0	453,7	2.9	110×10^{-3}

T'_m values for Moplen are close to those for sample H97,5 the value of γ for Moplen is about twice those for the high-yield samples. This implies that the thickening of the lamellae ($\gamma > 1$) during the crystallization at T_c [8] is more pronounced in the case of Moplen and could relate to a distribution of the thicknesses of the crystalline lamellae different from those for other samples, and hence to different behaviour during the heating run. Moreover, the presence of a multiple fusion peak in DSC curves of Moplen can be related to the occurrence of different crystallization phenomena (Fig. 5). In fact, Moplen samples partially crystallized at the same T_c for various times —corresponding to the two straight lines of the Avrami plot in Fig. 3 – show a unique melting peak for low crystallization times (primary crystallization) and a second peak at lower temperature only for longer times (secondary crystallization). Such results suggest that when polymers with configurational chain defects are allowed to crystallize isothermally at moderate undercooling values, molecules with lower stereoregularity give rise to crystalline regions with a degree of order smaller than that corresponding to the crystals of highly stereoregular chain segments [9].

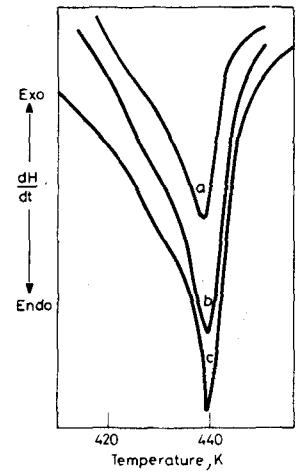

Fig. 5 DSC melting peaks of low-yield iPP (Moplen) after various crystallization times. (a) after 70 sec, (b) after 155 sec, (c) 600 sec

Nucleation control of crystallization rate

Assuming that the process of crystal growth (corresponding to the primary crystallization) is controlled by a mechanism of surface-coherent bi-dimensional nucleation, then in accordance with the kinetic theory of polymer crystallization [8] the temperature-dependence of the overall kinetic rate constant may be expressed by the relation:

$$\frac{1}{n}\log_{10} K_n = A_0 - \frac{\Delta F^*}{2.3\,RT_c} - \frac{\Delta \Phi^*}{2.3\,KT_c} \tag{3}$$

where A_0 is a constant (on the hypothesis that the density of primary nucleation at each T_c examined does not vary with time), ΔF^* is the activation energy for the transport of the molecules at the liquid–solid interface, K is the Boltzmann constant, and $\Delta \Phi^*$ is the energy of formation of a nucleus of critical dimensions, expressed as:

$$\Delta \Phi^* = \frac{4b_0 \sigma \sigma_e T_m}{\Delta H_f \Delta T} \tag{4}$$

In Eq. (4) b_0 is the distance between two adjacent fold planes, σ and σ_e are the free energies of formation per unit area of the lateral and folding surfaces of the crystals, and ΔH_f is the enthalpy of fusion.

The transport term ΔF^* is usually expressed as the activation energy of viscous flow according to the relation of William et al. [10]:

$$\Delta F^* = \frac{C_1 T_c}{C_2 + T_c - T_g} \tag{5}$$

where C_1 and C_2 are constants generally assumed equal to 17.2 kJ/mol and 51.5 K respectively, and T_g is the glass transition temperature. For all the samples examined $T_g = 260$ K has been used, in accordance with the literature data.

As shown in Fig. 6, plots of the quantity

$$\left[\frac{1}{n}\log_{10} K_n + \frac{F^*}{2.3\,RT_c}\right] \text{ vs. } \frac{T_m}{T_c \Delta T}$$

are straight lines whose slopes, according to (3) and (4), are given by the quantity

$$-\frac{4 b_0 \sigma \sigma_e}{2.3\,K \Delta H_f} \tag{6}$$

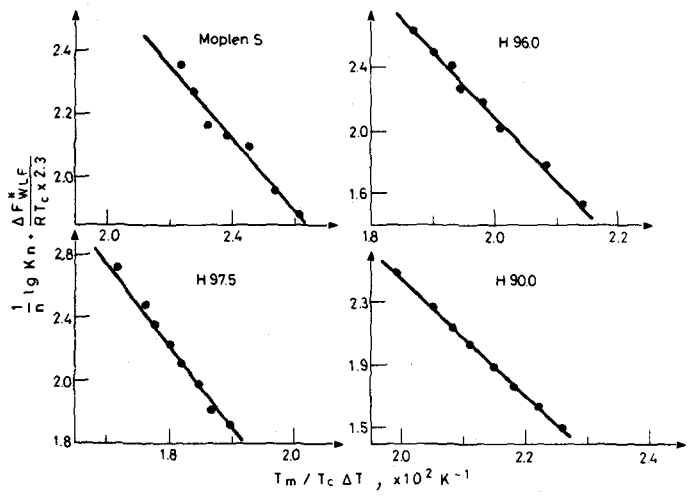

Fig. 6 Plots of the quantity $(1/n \log_{10} K_n + \Delta F^*_{WLF}/2.3\,RT_c)$ *vs.* $T_m/T_c\Delta T$, according to Eq (3) and (4), for various low- and high-yield iPP samples

Substitution of $b_0 = 0.525$ nm [11], $\Delta H_f = 209$ kJ/kg [4] and $\sigma = 0.1(b_0 \Delta H_f)$ [8 into Eq. (5): allows the surface energy of folding σ_e of iPP lamellar crystals to b calculated. Analogously, with the use of Eq. (4) the energy of formation of a nucleu of critical dimensions $\Delta\Phi^*$ has been calculated for different values of the undercoolin ΔT. The values of σ_e and $\Delta\Phi^*$ for the various iPP samples examined are reported i Table 3 and Fig. 7, respectively.

Both σ_e and $\Delta\Phi^*$ increase with the increase of the isotacticity index, while lowe values are observed for Moplen. Such behaviour may be mainly accounted for by th

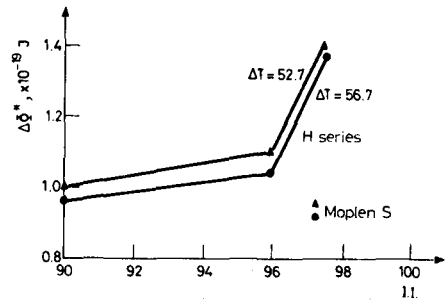

Fig. 7 Energy of formation of a nucleus of critical dimensions $\Delta\Phi^*$ at two different values of the undercooling ΔT as a function of the isotacticity index I.I. of low-yield and high-yield iPP samples.

amount and distribution of the configurational irregularities along the molecules of the various samples, and by the molecular weight distribution as a consequence of the different catalyst systems employed. The large variations observed in the values of σ_e for high-yield samples is probably to be ascribed to the fact that the fold surface of iPP crystals undergoes deep changes and becomes less regular as the content of stereoirregular sequences in the chains and/or the presence of uncrystallizable polymer increases.

Moreover, it is interesting to underline that a similar trend in $\Delta\Phi^*$ has also been observed in the melt crystallization of isotactic (propylene-1, butene) random copolymers [11] and for iPP fractions with different degrees of stereoregularity [2]. In fact, $\Delta\Phi^*$ was found to decrease with increasing butene content or with decreasing isotactic pentad concentration. These findings are in agreement with the trend observed for the values of the half-time of crystallization $t_{0.5}$ at constant ΔT, as shown in Fig. 3, i.e. the increase of the overall crystallization rates in the iPP samples with low isotacticity degrees under the same undercooling is to be ascribed to the lowering of the energy of formation of critical nuclei.

* * *

This work was supported by the "Progetto Finalizzato Chimica Fine e Secondaria" of C.N.R.

References

1 E. Martuscelli, M. Pracella and A. Zambelli, J. Polymer Sci., Phys. Ed., 18 (1980) 619.
2 L. Crispino, E. Martuscelli and M. Pracella, Polymer, in print.
3 M. Avella, E. Martuscelli and M. Pracella, Proceedings of Fourth National Conference on Calorimetry and Thermal Analysis, Catania, 1982.
4 J. Brandrup and E. H. Immergut, Polymer Handbook, Interscience Publication, New York, 1975, p. V-24.
5 H. D. Keith and F. J. Padden, J. Appl. Phys., 35 (1964) 1286.
6 L. Mandelkern, Crystallization in Polymers, McGraw-Hill, New York, 1964.
7 B. Wunderlich, Macromolecular Physics, Academic Press, New York, 1976, Vol. 2, p. 235.
8 J. D. Hoffmann, G. T. Davis and J. I. Lauritzen, in Treatise on Solid State Chemistry ed. by Hannay, Plenum Press, New York, 1976, Vol. 3, Ch. 7.
9 M. Pracella, Proceedings of Third National Conference on Calorimetry and Thermal Analysis, Genova, 1981.
10 H. L. Williams, R. F. Landel and J. D. Ferry, J. Am. Chem. Soc., 77 (1955) 3701.
11 L. Crispino, E. Martuscelli and M. Pracella, Makromol. Chem., 181 (1980) 1747.

Zusammenfassung – Das Kristallisations- und Schmelzverhalten von mit Hilfe verschiedener katalytischer Systeme (low- and high-yield) synthetisiertem isotaktischem Polypropylen (iPP) wurde durch Scanning-Kalorimetrie und optische Mikroskopie untersucht. Die isotherme Kristallisationsgeschwindigkeit der Schmelze hängt vom angewandten katalytischen System und vom Isotaktizitätsindex der Probe ab. Im Falle von "low-yield" iPP ergab die kinetische Auswertung des Gesamtprozesses nach Avramy Hinweise auf sekundäre Kristallisationsphänomene. Die Werte des Gleichgewichtsschmelzpunktes, der Keimbildungsenergie und der Oberflächenenergie der Faltung lamellarer iPP-Kristalle wurden nach der kinetischen Theorie der Polymerkristallisation berechnet. Unterschiede in diesen thermodynamischen Parametern, die für verschiedene iPP-Proben zu beobachten sind, wurden auf die Menge und den Typ der konfigurationellen Unregelmässigkeiten entlang der Ketten und auf Unterschiede in der Molekulargewichtsverteilung zurückgeführt.

Резюме – Методом ДСК и оптической микроскопии изучен процесс кристаллизации и плавления образцов изотактического полипропилена, синтезированного с различными катализаторами. Найдено, что скорость изотермической кристаллизации зависит от типа использованного катализатора и от индекса изотактичности образца. Однако, для низкотекучего изотактического полипропилена, анализ суммарного уравнения кинетики реакции, проведенного по Аврами, показал наличие вторичного процесса кристаллизации. Значения равновесной точки плавления, энергии образования центров кристаллизации и поверхностная энергия излома ламеллярных кристаллов изотактического полипропилена были вычислены на основе "кинетических теорий" кристаллизации полимеров. Наблюдаемое для различных образцов полимера изменение термодинамических параметров, было объяснено изменением степени и типа конфигурационных нарушений вдоль цепей и различиями в распределении молекулярного веса.